Regular Paper
J. Korean Inst. Electr. Electron. Mater. Eng.
Vol. 30, No. 9, pp. 546-550 September 2017
DOI: https://doi.org/10.4313/JKEM.2017.30.9.546
ISSN 1226-7945(Print), 2288-3258(Online)



# Ferroelastic Domain Wall Motions in Lead Zirconate Titanate Under Compressive Stress Observed by Piezoresponse Force Microscopy

**Kwanlae Kim**[1,2,a]

[1] Department of Engineering Science, University of Oxford, Oxford, United Kingdom
[2] Department of Materials Science and Engineering, Yonsei University, Seoul 03722, Korea

(Received August 7, 2017; Accepted August 14, 2017)

**Abstract:** Ferroelectric properties are governed by domain structures and domain wall motions, so it is of significance to understand domain evolution processes under mechanical stress. In the present study, *in situ* piezoresponse force microscopy (PFM) observation under compressive stress was carried out for a near-morphotropic PZT. Both 180° and non-180° domain structures were observed from PFM images, and their habit planes were identified using electron backscatter diffraction in conjunction with PFM data. By externally applied mechanical stress, needle-like non-180° domain patterns were broadened via domain wall motions. This was interpreted via phenomenological approach such that the total energy minimization can be achieved by domain wall motion rather than domain nucleation mainly due to the local gradient energy. Meanwhile, no motion was observed from curvy 180° domain walls under the mechanical stress, validating that 180° domain walls are not directly influenced by mechanical stress.

**Keywords:** Ferroelectric, Piezoresponse force microscopy, Domain structure, Compression

## 1. INTRODUCTION

Ferroelectrics have a very wide range of applications such as piezoelectric devices [1], random access memory [2], and capacitors [3]. In particular, there has been intensive research on piezoelectric microelectromechanical systems (MEMS) utilizing electromechanical coupling effect in ferroelectrics [4]. The properties of ferroelectrics including hysteresis curve and piezoelectric coefficients are governed by domain structure and domain wall motion [5,6]. Therefore, it is essential to understand domain evolution processes under electric field or mechanical stress in order to enhance the electromechanical coupling coefficient in MEMS devices.

Piezoresponse force microscopy (PFM) is one of the most used characterization techniques to observe ferroelectric domain structures [7–13]. PFM represents ferroelectric domain structures by distinguishing distinct polarization directions, so PFM can visualize complex domain patterns with both 180° and non-180° domain walls, which is the main advantage of PFM over other characterization techniques. There were previous works on PFM observation of ferroelectric domain evolution under electric field by using the scanning probeas a movable electrode [9,14]. Contrary to electrical loading, there has been relatively little work done on *in situ* PFM observation of ferroelastic domain evolution under mechanical loading.

In the present work, domain evolution process in a near-morphotropic PZT under compressive stress was observed

**a. Corresponding author; kwanlae.kim@daum.net**

using vertical PFM. This study experimentally reveals that 180° domain walls are not influenced by mechanical stress and broadening process of non-180° needle-like domain patterns. Finally, electron backscatter diffraction (EBSD) was used in conjunction with PFM to identify the crystallographic planes for the observed non-180° domain walls in PFM images.

## 2. METHOD FOR EXPERIMENT

Polycrystalline soft PZT near morphotropic phase boundary (MPB), distributed by APC international and designated PZT-855, was used. This particular material was chosen because both tetragonal and rhombohedral phases can coexist, facilitating polarization switching between <100> and <111> directions under externally applied mechanical stress. Therefore, domain wall motions are likely to be easily captured by PFM images during compression. A cuboid sample with 2×4×5 $mm^3$ dimensions was prepared and one of the 4×5 $mm^2$ faces was polished for PFM observation.

Vertical PFM was performed using a Veeco Dimension 3100 nanoscope. In PFM, alternating voltage is applied through the scanning probe to the sample, inducing mechanical oscillation in the sample surface via converse piezoelectric effect. The vertical component of the surface displacement is detected by the contacting scanning probe, and the vertical motion of the scanning probe is detected by the reflected laser beam from the cantilever onto the photodetector. In the present experiment, the piezoelectric response signal is in the form of $A\cos\phi/V_{ac}$, where $A$ is the amplitude, $\phi$ is the phase of the piezoelectric response signal, and $V_{ac}$ is the alternating voltage applied to the scanning probe. Because each domain generates unique $A$ and $\phi$, complex domain patterns can be effectively exposed by PFM technique. Bruker SCM-PIC scaning probes were used, and in particular, 160~200 kHz driving frequency was used to induce contact resonance [15] in the scanning probe.

A micromechanical test rig (Deben Ltd., UK) was used for *in situ* PFM observation under compressive stress (Figures 1(a)~(b)). The test rig was connected to the sample stage in the AFM, enabling precision position control of the test rig and the sample. As shown in Fig. 1(c), the compressive stress was applied along the $x_2$ direction, and PFM scan was conducted on the top of the PZT sample surface. In the present experiment, a strain

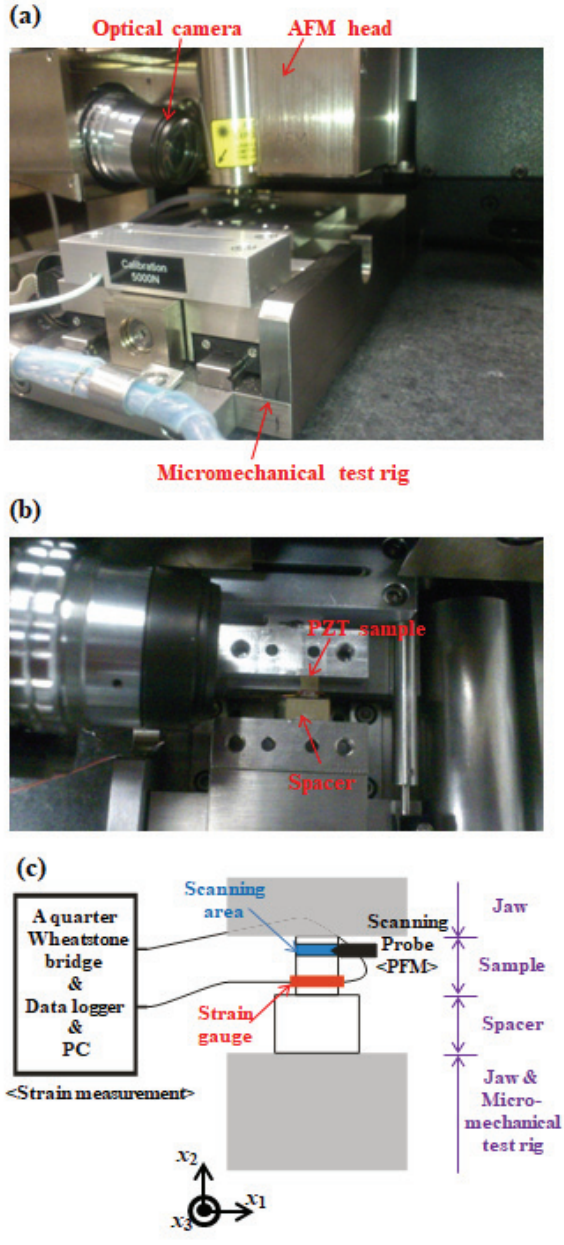


**Fig. 1.** (a) A micromechanical test rig under AFM head, (b) top view of the PZT sample between the jaws in the test rig, and (c) schematic of the experimental set-up for *in situ* PFM observation of PZT under mechanical loading.

gauge was positioned on the same surface of the PZT sample in which the PFM scan was performed to monitor the macroscopic strain parallel to the loading direction. A preliminary test was performed by applying stress up to a 0.05% stain to the sample in order to confirm that no bending was taking place on the PZT sample surface and PFM scan was reliably performed without severe mechanical oscillation by the test rig. PFM scans were performed four times: before mechanical loading, under mechanical loading (approximately 0.12%, and 0.13% strain), and after unloading. Even after removing externally applied mechanical stress, the measured strain was about 0.05% due to a residual strain present in the PZT sample.

Finally, EBSD was used to identify the crystallographic planes for the non-180° domain walls observed in the PFM images. EBSD measurements were carried out using an Evo LS 15 environmental scanning electron microscopy (ESEM).

## 3. RESULTS AND DISCUSSIONS

Figures 2(a)~(c) show the EBSD inverse pole figure, AFM topography image, and vertical PFM image for the grain marked "Gr1". The grain "Gr1" found using AFM was retraced by scanning electron microscopy using the instrument coordinate system. In EBSD, Kikuchi patterns are generated from the diffraction of electrons by lattice planes, and the three Euler angles can be obtained. Thus, the crystallographic orientation for the grain "Gr1" can be identified as shown in Fig. 2(c). The crystallographic planes corresponding to the non-180° domain walls in Fig. 2(c) were identified by matching {100} and {110} planes to the domain wall orientatios in the PFM images. To achieve energy minimization, a domain wall must satisfy electrical and mechanical compatibility conditions [16]. For a pair of domains $i$ and $j$ with the strain states $\varepsilon_i$, $\varepsilon_j$, and polarization vectors $\mathbf{p}_i$, $\mathbf{p}_j$, the interface normal vector, $\mathbf{n}$, enabling compatible arrangement of domains, must satisfy [16]

$$\epsilon_i - \epsilon_j = \frac{1}{2}(\mathbf{a}\otimes\mathbf{n} + \mathbf{n}\otimes\mathbf{a}), \quad (1)$$

$$(\mathbf{p}_i - \mathbf{p}_j) \cdot \mathbf{n} = 0, \quad (2)$$

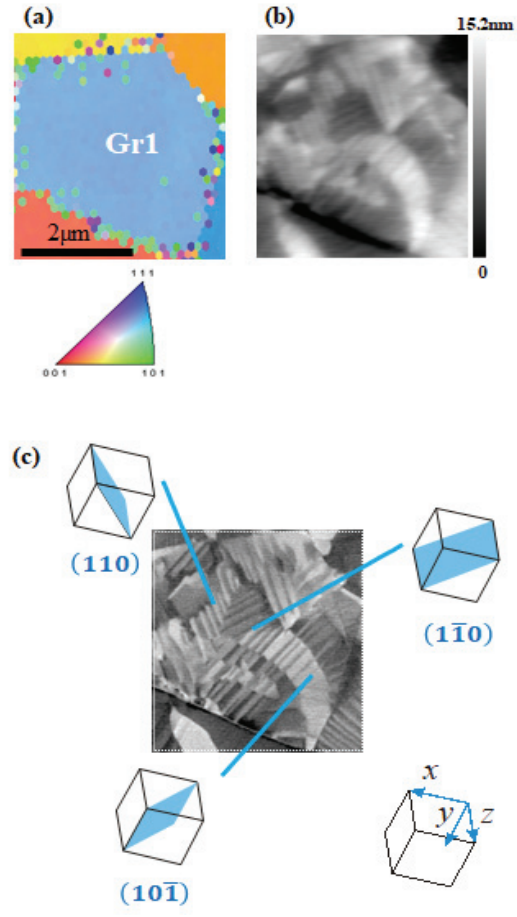


**Fig. 2.** Characterization of the grain "Gr1" through (a) EBSD inverse pole figure, (b) AFM topography image, and (c) the crystallographic orientation for the grain "Gr1" and the crystallographic planes for the non-18° domain walls in the PFM image were identified using Kikuchi patterns in EBSD.

where $\mathbf{a}$ can be any vector satisfying Equation (1). A unique domain wall orientation, $\mathbf{n}$, can be obtained by solving Equations (1) and (2), except for the special case $\epsilon_i = \epsilon_j$. In this case, Equation (1) can be solved by setting $\mathbf{a} = 0$, and a continuous set of solutions for $\mathbf{n}$ can be generated from Equation (2). Such a special case can be found from 180° domain structures in which strain states are identical across the domain walls. Therefore, a 180° domain wall has no habit plane and appears as a curvy line on a sample surface. Contrary to 180° domain walls, non-180° domain walls can be formed at certain crystallographic planes. Spontaneous polarization directions in PZT are <100> and <111> in tetragonal and

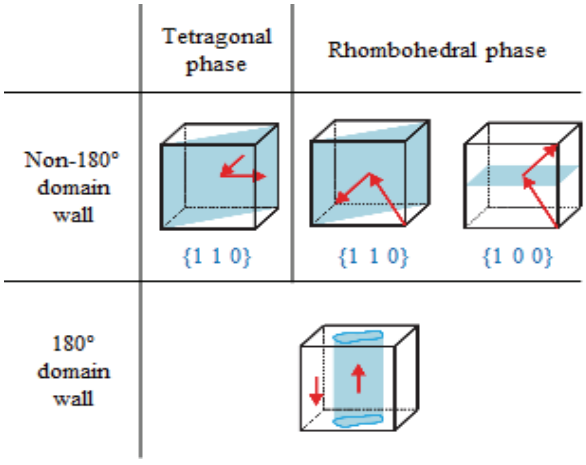


**Fig. 3.** Compatible non-180° and 180° domain wall in tetragonal and rhombohedral phases.

rhombohedral phases, respectively, so electrically and mechanically compatible non-180° domain walls are formed at {110} planes in tetragonal phase, and at {110} and {100} planes in rhombohedral phase (Fig. 3) [17]. The identified crystallographic planes for the observed non-180° domain walls are shown in Fig. 2(c). However, the phase of the grain "Gr1" cannot be identified since {110} planes can be present in both tetragonal and rhombohedral phases. Therefore, analysis for the EBSD data was not further carried out in the present study. Nevertheless, the analysis method combining PFM and EBSD data can be applied to the other ferroelectric materials in which the phase is known.

Domain evolution processes for the grain "Gr1" observed by PFM technique under compressive stress are represented in Fig. 4. Domain patterns corresponding to before loading, under 0.12% strain, under 0.13% strain, and after unloading are shown in Figs. 4(a)~(d), respectively. The schematics simplifying the domain patterns corresponding to before loading and under 0.134% strain are given in Figs. 4(e)~(f), respectively. First of all, typical non-180° needle-like domain patterns can be observed from Fig. 4(a). Figures 4(b)~(c) show that when the strain increased to 0.12% and 0.13%, the needles were broadened via domain wall motion by externally applied compressive stress. Such a domain wall motion occurs because individual polarization switching is induced to minimize

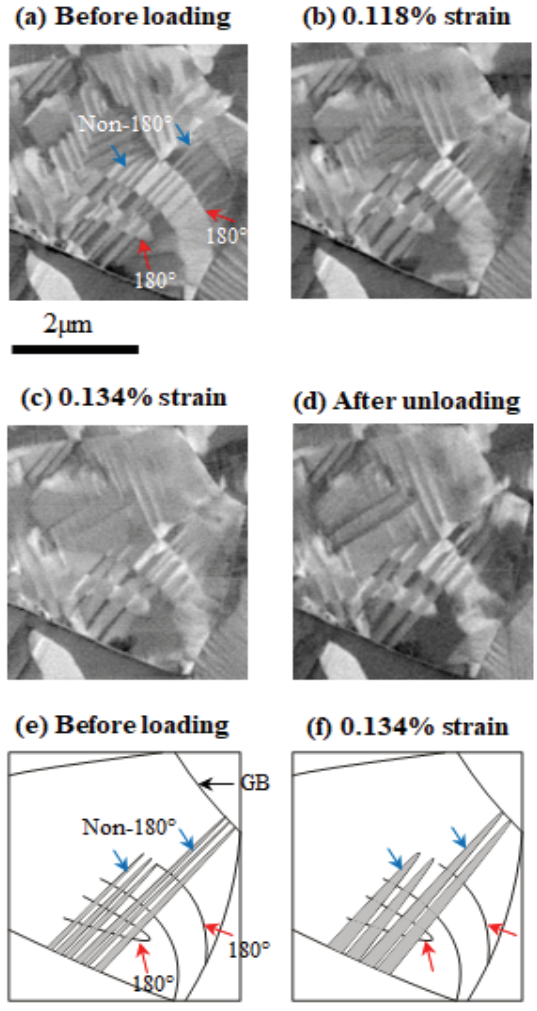


**Fig. 4.** (a)~(d) PFM images showing non-180° domain wall motion under compressive loading and (e)~(f) Two schematics depict the broadening process of needle-like domain structures.

the total energy with respect to the externally applied stress. According to the phenomenological approach, the total free energy of ferroelectrics can be represented as [18]

$$F_{tot} = f_e + f_{es} + f_{dip} + f_g + f_S \quad (3)$$

where $f_e$ is the elastic strain energy, $f_{es}$ is the electrostrictive energy, $f_{dip}$ is the free energy of dipole-dipole interaction, $f_g$ is the local gradient energy, and $f_S$ is the free energy due to the externally applied stress. When switching a polarization direction by externally applied

stress, domain nucleation is energetically unfavorable due to an increase in $f_g$. Thus, domain switching takes place via domain wall motion rather than domain nucleation. Meanwhile, curvy lines marked "180°" can be seen in Fig. 4(a). According to the compatibility theory mentioned earlier, these curvy walls are assumed to be 180° domain walls. Under compressive stress, no noticeable motion in these 180° domain walls occurred. This is because the strain states of the domains are identical across 180°, so the total energy of the material is not reduced via 180° domain wall motion under mechanical stress.

## 4. CONCLUSION

The domain structures and their evolution processes under the externally applied compressive stress in a near-morphotropic PZT ceramic were observed using vertical PFM. A micromechanical test rig was installed under AFM head enabling *in situ* observation under compressive loading. The crystallographic planes for the observed non-180° domain walls were identified using PFM and EBSD data. Both 180° and non-180° domain walls were observed from the PZT sample surface. By externally applied mechanical stress, domain switching in non-180° domain occurred via the broadening process in the needle-like domain patterns. Polarization switching via domain wall motion was favored than domain nucleation because domain nucleation involves energetically unfavorable local gradient energy. Contrary to non-180°, any noticeable motion was not observed from the curvy 180° domain walls since the total free energy is not minimized via 180° domain switching by mechanical stress.

## REFERENCES

[1] T. D. Nguyen, N. Deshmukh, J. M. Nagarah, T. Kramer, P. K. Purohit, M. J. Berry, and M. C. McAlpine, *Nat. Nanotechnol.*, **7**, 587 (2012). [DOI: http://dx.doi.org/10.1038/NNANO.2012.112]

[2] N. Izyumskaya, Y. I. Alivov, S. J. Cho, H. Morkoç, H. Lee, and Y. S. Kang, *Crit. Rev. Solid State Mater. Sci.*, **32**, 111 (2007). [DOI: http://dx.doi.org/10.1080/10408430701707347]

[3] G. H. Haertling, *J. Am. Ceram. Soc.*, **82**, 797 (1999). [DOI: http://dx.doi.org/10.1111/j.1151-2916.1999.tb01840.x]

[4] C. Liu, *Foundations of MEMS* (Pearson Education, Inc., New Jersey, 2006), Chap. 7.

[5] V. Nagarajan, A. Roytburd, A. Stanishevsky, S. Prasertchoung, T. Zhao, L. Chen, J. Melngailis, O. Auciello, and R. Ramesh, *Nat. Mater.*, **2**, 43 (2003). [DOI: http://dx.doi.org/10.1038/nmat800]

[6] G. Arlt, *Ferroelectrics*, **104**, 217 (1990). [DOI: http://dx.doi.org/10.1080/00150199008223825]

[7] S. V. Kalinin, B. J. Rodriguez, S. Jesse, J. Shin, A.P. Baddorf, P. Gupta, H. Jain, D. B. Williams, and A. Gruverman, *Microsc. Microanal.*, **12**, 206 (2006). [DOI: http://dx.doi.org/10.1017/S1431927606060156]

[8] S. V. Kalinin and N. Balke, *Adv. Energy Mater.*, **22**, E193 (2010). [DOI: http://dx.doi.org/10.1002/adma.201001190]

[9] A. Gruverman, O. Auciello, and H. Tokumoto, *Annu. Rev. Mater. Sci.*, **28**, 101 (1998). [DOI: https://doi.org/10.1146/annurev.matsci.28.1.101]

[10] A. N. Morozovska, S. V. Svechnikov, E. A. Eliseev, S. Jesse, B. J. Rodriguez, and S. V. Kalinin, *J. Appl. Phys.*, **102**, 114108 (2007). [DOI: http://dx.doi.org/10.1063/1.2818370]

[11] S. V. Kalinin, A. Rar, and S. Jesse, *IEEE Trans. Ultrason. Ferroelectr. Freq. Control.*, **53**, 2226 (2006). [DOI: https://doi.org/10.1109/TUFFC.2006.169]

[12] E. Soergel, *Appl. Phys. B*, **81**, 729 (2005). [DOI: https://doi.org/10.1007/s00340-005-1989-9]

[13] E. Soergel, *J. Phys. D: Appl. Phys.*, **44**, 464003 (2011). [DOI: https://doi.org/10.1088/0022-3727/44/46/464003]

[14] C. H. Ahn, T. Tybell, L. Antognazza, K. Char, R. H. Hammond, M. R. Beasley, O. Fischer, and J. M. Triscone, *Science*, **276**, 1100 (1997). [DOI: https://doi.org/10.1126/science.276.5315.1100]

[15] S. Jesse, S. V. Kalinin, R. Proksch, A. P. Baddorf, and B. J. Rodriguez, *Nanotechnology*, **18**, 435503 (2007). [DOI: https://doi.org/10.1088/0957-4484/18/43/435503]

[16] Y. C. Shu and K. Bhattacharya, *Philos. Mag. B*, **81**, 2021 (2001). [DOI: http://dx.doi.org/10.1080/13642810108208556]

[17] A. J. Moulson and J. M. Herbert, *Electroceramics : Materials, Properties, Applications* (John Wiley & Sons Ltd., Chichester, 2003) Chap. 2.

[18] F. Xue, X. S. Gao, and J. M. Liu, *J. Appl. Phys.*, **106**, 114103 (2009). [DOI: http://dx.doi.org/10.1063/1.3259374]